Journal of Theoretical Biology 341 (2014) 9–16

Contents lists available at ScienceDirect

Journal of Theoretical Biology

journal homepage: www.elsevier.com/locate/yjtbi

Wind and gravity mechanical effects on leaf inclination angles

Loïc Tadrist [a,b,*], Marc Saudreau [b], Emmanuel de Langre [a]

[a] École Polytechnique, Laboratoire d'hydrodynamique, 91128 Palaiseau, France
[b] INRA, Physique et Physiologie intégratives de l'arbre fruitier et forestier, 63100 Clermont-Ferrand, France

HIGHLIGHTS

- A biomechanical model of Leaf Inclination Angle Distribution (LIAD) is proposed.
- Self-weight and wind loading are considered.
- Leaf flexibility impacts strongly Leaf Inclination Angle Distribution.
- A change in leaf flexibility or external loading may change light interception.

ARTICLE INFO

Article history:
Received 17 May 2013
Received in revised form
25 July 2013
Accepted 18 September 2013
Available online 25 September 2013

Keywords:
Leaves
Inclination angle
Biomechanics
Flexibility
Wind

ABSTRACT

In a tree, the distribution of leaf inclination angles plays an important role in photosynthesis and water interception. We investigate here the effect of mechanical deformations of leaves due to wind or their own weight on this distribution. First, the specific role of the geometry of the tree is identified and shown to be weak, using models of idealized tree and tools of statistical mechanics. Then the deformation of individual leaves under gravity or wind is quantified experimentally. New dimensionless parameters are proposed, and used in simple models of these deformations. By combining models of tree geometry and models of leaf deformation, we explore the role of all mechanical parameters on the Leaf Inclination Angle Distributions. These are found to have a significant influence, which is exemplified finally in computations of direct light interception by idealized trees.

1. Introduction

Among leaf geometrical traits, the leaf inclination angle, defined as the leaf orientation with respect to the vertical axis, is of primary importance in plant ecology as it directly drives radiation interception by canopies and thus impacts gas exchanges, photosynthetic activity level and related processes within canopies. The Leaf Inclination Angle Distribution (LIAD) is commonly described in a given tree through a probability distribution function $p(\varphi)$, where φ is the angle between the leaf normal direction and the vertical axis (Falster and Westoby, 2003; Wang et al., 2007). For instance, when the sun is at zenith, the direct light interception by a canopy, I_0, is commonly modeled as (Monsi and Saeki, 2005; Pisek et al., 2013)

$$\ln\left(\frac{I_0}{I_H}\right) = -A\left[1 - \int_0^{\pi/2} p(\varphi)\cos\ \varphi\ \mathrm{d}\varphi\right], \tag{1}$$

where I_H is the light intensity at the top of the canopy and A is a function of the leaf density profile. Clearly the probability density function of the leaf orientation, $p(\varphi)$, has a strong effect on the interception of light by a canopy.

The LIAD may be defined in several ways, considering that a leaf may be curved and even if not curved, tilted across its mid-rib axis. For the sake of simplicity, we shall hereafter use as inclination angle, ϕ, the angle between the vertical axis and the base-tip axis of the lamina (Fig. 1a). Note that ϕ does now vary from 0 to π, contrary to other definitions such as in Eq. (1) where φ varies from 0 to $\pi/2$. The distributions $P(\phi)$ and $p(\varphi)$ are simply linked by $p(\varphi) = P(\varphi) + P(\pi - \varphi)$. In the following, the probability density function $P(\phi)$ will be referred to as the Leaf Inclination Angle Distribution (LIAD). Fig. 1c and e shows a typical LIAD (Falster and Westoby, 2003; Falster, 2012), one among the immense variety that exists in nature. They may differ by the location of the peak, the width of this peak or even by their general shape, see for instance Falster and Westoby (2003) for typical examples.

Observed LIADs are highly variable between species and can change over time along the growing season or according to abiotic and biotic stresses (Pisek et al., 2013; Falster and Westoby, 2003).

* Corresponding author at: École Polytechnique, Laboratoire d'hydrodynamique, 91128 Palaiseau, France. Tel.: +33 674100203.
E-mail address: loic.tadrist@ladhyx.polytechnique.fr (L. Tadrist).

0022-5193/$ - see front matter © 2013 Elsevier Ltd. All rights reserved.
http://dx.doi.org/10.1016/j.jtbi.2013.09.025

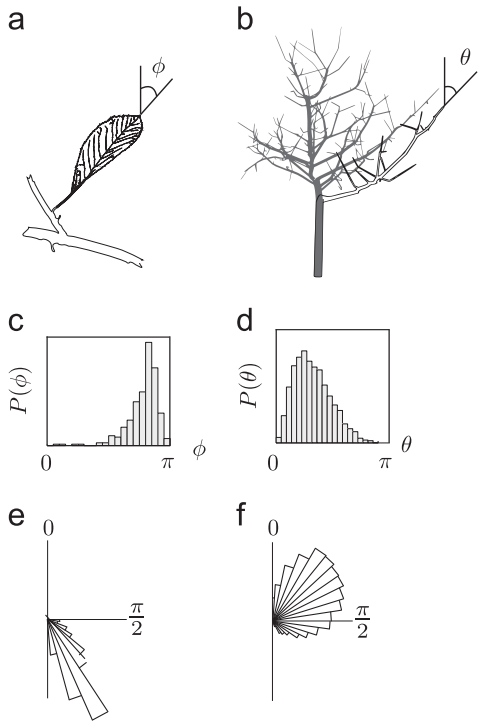

Fig. 1. (a) Definition of the leaf inclination angle, ϕ. (b) Definition of the branch inclination angle, θ. (c) Example of LIAD (data by Falster (2012)), the same LIAD is also plotted in polar representation in (e). (d) Example of BIAD (data by Rodriguez et al. (2012)), the same BIAD is also plotted in polar representation in (f). The distributions are shown with arbitrary amplitudes.

This variability is probably due to both physical and biological factors: the tree architecture (through the inclination of branches), the deformation of the petioles, which itself depends on turgor pressure, phototropism, growth history and even instantaneous reactions to stimuli. To account for this huge variability numerous functions such as spherical, ellipsoidal or Beta distributions are commonly used (Campbell, 1986; Wang et al., 2007; Pisek et al., 2011). However these functions do not take into account any of the factors listed above. We expect that including some of these factors into a model can account simply for this variability. We shall focus hereafter on the combined role of the first two of the above list, namely the tree architecture and the elastic deformation of petioles under gravity or wind loading. The first one is mainly geometrical and the second mechanical.

We define at this step the Branch Inclination Angle Distribution (BIAD), which describes the orientation of the shoots supporting the leaves with the vertical axis, Fig. 1b. Fig. 1d and f shows a typical BIAD corresponding to a specific walnut tree (Rodriguez et al., 2012). Modeling the BIAD requires some knowledge of the tree geometry. Successful models, using simple iterating branching laws, have been used for tree vibration (Rodriguez et al., 2012) and for tree fracture (Lopez, 2011; Eloy, 2011). These models are based on a branching angle and allometric laws only.

On the other hand, the elastic deformation of a petiole has been considered by Vogel (1989) and Niklas (1999), using simple beam models. They showed that the static and dynamic deformations of the whole leaf are concentrated in the petiole for most leaves. This idealized model of leaf deformation is not adapted when the lamina is more flexible than the petiole or for complex geometries such as pinnate leaves and sessile leaves. Nevertheless, models considering the lamina as rigid and the petiole as flexible are efficient in most applications (Niklas, 1992; Niinemets and Fleck, 2002).

The aim of the present paper is to combine simple models of branch orientation with models of petiole deformation under external loading, in order to understand and ultimately predict some of the existing features of leaf inclination angle distributions. More precisely we seek to clarify the respective role of these two factors, geometrical or mechanical, affecting LIADs.

Considering the large number of branches and leaves we shall use standard methods of statistical physics to build the probability density functions. In Section 2, the Branch Inclination Angle Distribution is built for idealized two-dimensional and three-dimensional trees. In Section 3, a model is proposed to describe the deformation of a leaf under two types of loads: that induced by gravity and that induced by wind. In Section 4 these results are combined to derive LIADs and their variations with parameters. The possible effects on a global quantity such as the light interception are also discussed.

2. Branch inclination angle

2.1. The two-dimensional tree

We seek to establish first the role of tree geometries on inclination angles of branches which hold leaves. To do so we use a description based on the assumption of an iterative branching process. This is similar in principle to the models used by Rodriguez et al. (2008), Lopez (2011) or Eloy (2011) recently. The simplest model, referred hereafter as the 2D tree model, is illustrated in Fig. 2a. Here, the geometry results from a series of n iterations where the end segments of the tree are prolongated by two daughter branches, emerging with an angle θ_0 from each mother branch. As only inclinations are involved no other information is needed on length or diameter of the branches (see Rodriguez et al., 2008; Lopez, 2011).

As the BIAD describes the inclination angle of the shoots supporting leaves, we focus our analysis on the branches of the ultimate order of the tree, n. Elementary calculus shows that the

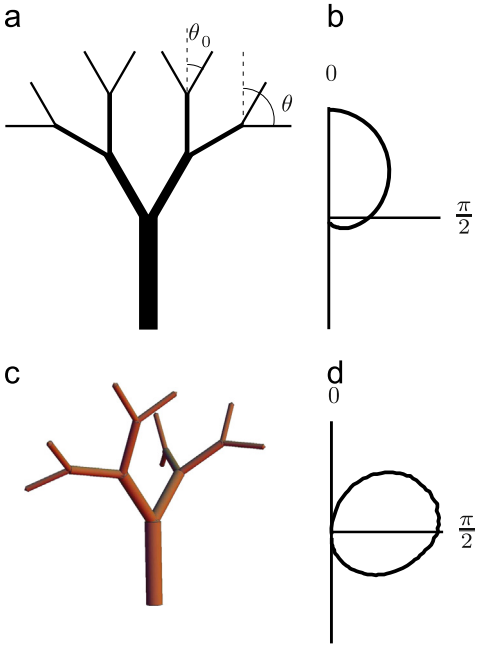

Fig. 2. Iterative idealized branched trees. (a) A two-dimensional tree, (b) the corresponding BIAD, Eq. (3), with the number of iteration n is equal to 4, for a branching angle $\theta_0 = \pi/6$. (c) A three-dimensional tree, (d) the corresponding BIAD obtained by numerical simulation with the same values of n and θ_0 by averaging over 10^5 trees.

inclination varies between $\theta=0$ and $\theta=n\theta_0$ depending on the location of the branches. The probability that a branch of order n has an inclination angle $\theta=k\theta_0$, n and k being integers, is noted $P_n(k\theta_0)$. The iteration law that defines this distribution reads

$$2P_{n+1}(k\theta_0)=P_n[(k-1)\theta_0]+P_n[(k+1)\theta_0], \tag{2}$$

with $P_{n+1}(\theta_0)=P_n(0)+P_n(2\theta_0)/2$ and $P_{n+1}(0)=P_n(\theta_0)/2$. Considering that the number of iterations n is generally large, say larger that 5 and up to 10 (Lopez, 2011), we may use elementary tools of statistical physics, see for instance, p. 23, Kittel (2004), to derive an approximation of the BIAD as

$$P_n(\theta)=\frac{1}{\theta_0}\sqrt{\frac{2}{n\pi}}e^{-\theta^2/2n\theta_0^2}. \tag{3}$$

Note that θ varies here continuously and is not restricted to the discrete values $\theta=k\theta_0$. Fig. 2b illustrates that the BIAD is a simple Gaussian peaked at $\theta=0$ and with a standard deviation, $\sigma=\theta_0\sqrt{n}$, depending on both the branching angle and the number of iterations. A comparison with the BIAD of a real tree, Fig. 1f, immediately shows that the present 2D model fails to capture the position of the peak of the distribution, clearly non-zero in practice.

2.2. The three-dimensional tree

To improve the model, we include now at each branching point a random rotation around the axis of the mother branch. This generates a full three-dimensional tree as illustrated in Fig. 2c. The corresponding distribution of inclination angles may not be analytically derived as it results itself from a random process. We numerically generate 10^4 random trees for a given set of parameters θ_0 and n, and average their BIADs to obtain a reference distribution, Fig. 2d. It significantly differs from that of the 2D approximation and is no more peaked at $\theta=0$. In fact the 2D model was biased by an excessive role of the vertical direction, thus favoring the $\theta=0$ angle. By systematically exploring the effect of n, we find a weak dependence of the number of iterations. These distributions are fitted with Gaussian shapes

$$P(\theta)\propto e^{-[(\theta-\mu)^2/2\sigma^2]}, \tag{4}$$

where the peak position, μ, and the standard deviation, σ, are found to depend only on the branching angle θ_0. Note that for the sake of clarity, we have omitted the normalization factor in Eq. (4) by using the notation "$\propto$", meaning that P is proportional to the right-hand side of the equation. By systematically varying θ_0, from 0 to $\pi/3$, we find that the peak position and the standard deviation are well approximated by

$$\mu=\frac{\pi}{2}\sin\left(\frac{3\theta_0}{2}\right) \quad \text{and} \quad \sigma=\frac{\pi}{4}\sin\left(\frac{3\theta_0}{2}\right). \tag{5}$$

This 3D model has the ability to represent a BIAD that is not peaked at $\theta=0$, contrary to the 2D model. Note that, since $3\theta_0<\pi$, the peak of the distribution is never larger than $\pi/2$. We may therefore directly state that geometrical effects are probably not responsible for well off-centered distributions of Leaves Inclination Angle Distribution (LIAD) such as that of Fig. 1c, near $3\pi/4$.

We apply the model defined by Eqs. (4) and (5) to derive the BIAD of the walnut tree, Fig. 3. From the digitized geometry of the walnut Fig. 3a, we compute the average branching angle, which is found equal to $\theta_0/\pi=0.26$. This angle is then used to predict the BIAD. Fig. 3b shows that the model predicts reasonably well the Branch Inclination Angle Distribution, using only the value of the branching angle.

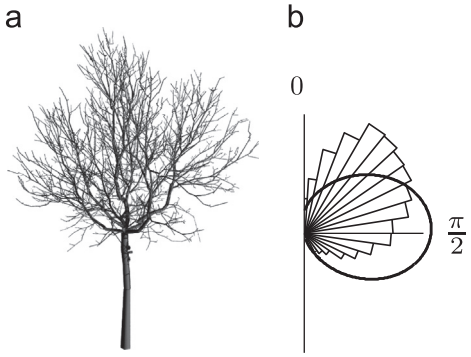

Fig. 3. (a) Digitized walnut geometry (Rodriguez et al., 2008). (b) Polar representation of the walnut BIAD (bars) and theoretical prediction (continuous line), Eqs. (4) and (5).

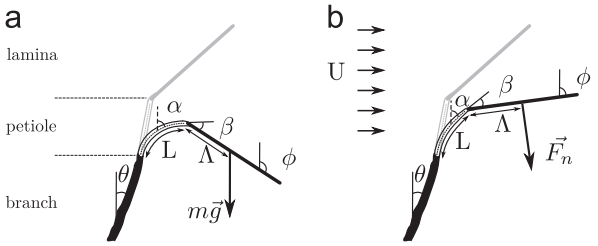

Fig. 4. Schematic view of the deformation of a leaf under external loading: (a) weight of the lamina and (b) wind forces. Also shown are the variables used in this section.

3. Local models of flexibility

We now consider the effect of flexibility at the scale of the individual leaf for different types of loading. Models that we build in this section will then be used to derive the inclination angles at the scale of the whole tree, by combination with the results of the preceding section.

3.1. Flexibility under gravity loading

The parameters involved in the local deformation of a leaf under gravity are the weight of the lamina, mg, the length of the leaf, 2Λ, the bending rigidity of the petiole, EI, and the length of the petiole, L (Fig. 4a). Elementary dimensional analysis shows that these parameters may be combined in an elasto-gravity number

$$E_G=\frac{\Lambda Lmg}{EI}, \tag{6}$$

which scales the loading by gravity on the lamina with the stiffness of the petiole, and therefore the potential deformation. Note that we have used the length L in place of $L+\Lambda$ in Eq. (6), for the sake of simplicity, without loss of generality. In all the cases we show further in the paper that L and Λ are of the same order of magnitude, so that our choice does not introduce a bias in the analysis of results. For leaves with $\Lambda\gg L$, using $L+\Lambda$ or even simply Λ would be appropriate. More generally, if the leaf mass distribution is not uniform, the proper length parameter is $L+L_G$ where L_G is the distance from the base of the lamina to the center of mass of the lamina. We estimated this elasto-gravity number on several species mainly of fruit trees, by measuring on sets of six leaves the parameters given above. To measure the petiole flexibility (EI), the difference is made between the curvature of a petiole with and without end load. The results are summarized in Table 1 showing that the elasto-gravity number typically ranges from 0.1 to 2, indicating that small or large deformation induced by gravity can be expected depending on that parameter.

Table 1
Table of parameters.

Symbols	Parameters
θ	Branch inclination angle
ϕ	Leaf inclination angle
ψ	Leaf azimuth angle
θ_0	Branching angle
n	Branching level
Λ	Half length of the lamina
L	Length of the petiole
m	Lamina mass
g	Gravity
EI	Bending stiffness
ρ	Air density
U	Wind velocity
C_N	Drag coefficient normal to the leaf
S	Leaf area
β	Angle between the petiole and the lamina
E_G	Elasto-gravity number
C_Y	Cauchy number
μ, Φ	Peak position (BIAD, LIAD)
σ, Σ	Width of the peak (BIAD, LIAD)
P	Inclination angle distribution
I_H	Light at the top of the canopy
γ	Solar inclination angle
I	Light intercepted
C	Light interception ratio
C_∞	Limit light interception ratio

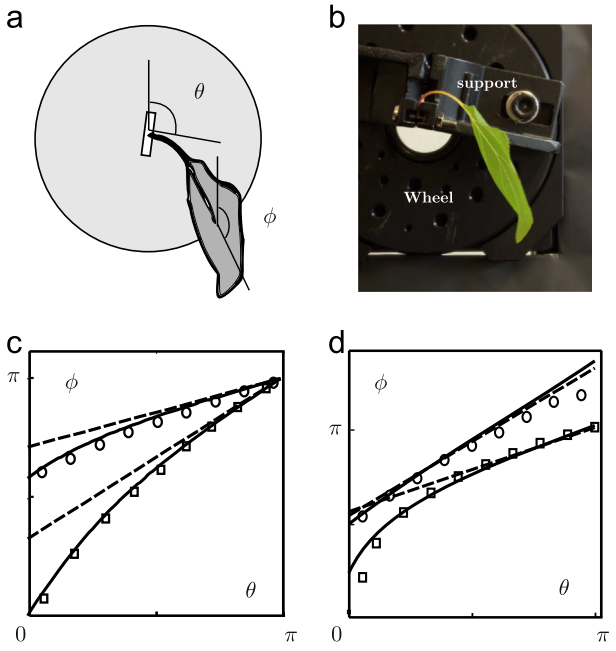

Fig. 5. (a) Sketch of the experiment. (b) Image taken from the experiment. (c) Results on artificial leaves (□) Model 1 and (○) Model 2. (d) Results on actual leaves (□) Apricot and (○) Ficus. (c) and (d) the solid line is the elastica model and the dashed line is the analytical approximation.

To quantify the deformation of the leaf system due to gravity, an experiment is designed as sketched in Fig. 5a. A leaf is clamped at the base of its petiole and the angle of clamping, θ, is progressively increased. The resulting position of the leaf is recorded with a camera, fitted with a macro lens of focal length 30 mm. The captured image, see Fig. 5b for an example, is then processed to extract the leaf inclination, ϕ, regardless of any reference position. Two types of leaves are tested: artificial leaves made of a plastic sheet for the lamina and an optic fiber for the petiole and tree leaves (*Ficus Benjamina* and *Prunus Armeniaca* 'Précoce de Saumur'). Table 3 gathers the characteristics of the tested leaves, including the angle between the petiole and the lamina, β. Fig. 5c and d shows the measured inclination angle, ϕ, as a function of the clamping angle θ.

To relate these results with the characteristics of the petiole, standard models from elasticity may be used. Considering the possible large deformation of the petiole, we use a fully non-linear formulation of the equilibrium equation, and do not assume that the petiole is horizontally inserted. The equation for the local angle of the petiole, α (Fig. 1b), reads (Salençon, 2001)

$$EI\frac{d^2\alpha}{ds^2} = -mg\ \sin\ \alpha, \tag{7}$$

where s is the curvilinear coordinate. In a dimensionless form, using $\bar{s} = s/L$ this reads

$$\frac{d^2\alpha}{d\bar{s}^2} = -E_G\frac{L}{\Lambda}\ \sin\ \alpha. \tag{8}$$

The boundary conditions at the branch side and the lamina side are $\alpha = \theta$ and $d\alpha/d\bar{s} = E_G\ \sin(\alpha+\beta)$ respectively. These equations are more general than those used by Niklas (1992), who considered the lamina as a point load at the end of the petiole and differ from those of Niinemets and Fleck (2002) by the non-linear terms, but considering only here a uniform mass distribution and a rigid lamina.

The solution of Eq. (8) involves elliptic integrals, but with a non-trivial boundary condition at $\bar{s} = 1$. We solve it numerically combining a standard Runge–Kutta procedure in space with a shooting technique to satisfy the branching condition. An approximate solution may also be given in the limits when $\Lambda \gg L$, large leaf or short petiole, and $\phi \approx \pi$, large inclination angle. The solution reads simply $\alpha(\bar{s}) = \theta + \bar{s}E_G(\pi - \phi + \beta)$ so that

$$\phi = \frac{\theta+\beta+\pi E_G}{1+E_G}. \tag{9}$$

Fig. 5c shows the experimental evolution of the inclination angle of artificial leaves, ϕ, as a function of inserting angle θ, in comparison with the models discussed above. Clearly the full mechanical model, Eq. (7), captures well the evolution of the inclination angle. The simplified model, Eq. (9), gives the main trends: ϕ increases with θ and tends to π for high values of E_G. For the real leaves, Fig. 5d, with a large angle β between the petiole and the lamina, the comparison shows the same trends. We shall, in the following section, use the simplified formula, Eq. (9), which allows analytical derivations.

3.2. Flexibility under wind loading

A similar approach may be undertaken for deformation induced by wind. The static load induced by wind on the leaf depends on the dynamic pressure, ρU^2, on the leaf area, S, proportional to Λ^2, and on the angle between the leaf and the wind velocity (de Langre, 2008). Consequently, the dimensionless number that scales the deformation induced by wind on the leaf is the Cauchy number (de Langre, 2008), defined here as

$$C_Y = \frac{\rho U^2 \Lambda^3 L}{EI}. \tag{10}$$

This number may be estimated, for winds of 0.1 m/s and 10 m/s, for all the leaves of the species analyzed above. Table 2 shows that Cauchy numbers, for such velocities range from 10^{-4} to 10^2. For $C_Y > 1$, significant deformation under wind may be expected.

An experiment is designed to explore the effect of wind loading on the deformation of a single leaf. Artificial leaves, as in the previous experiment, are placed in a wind tunnel, Fig. 6a (Lemaitre et al., 2005). Two leaves are considered with $L = 2.7$ cm, $\Lambda = 5.5$ cm,

Table 2
Typical values of the elasto-gravity number, E_G, and the Cauchy number, C_Y, at 0.1 m/s and 10 m/s. Only mean values for the set of leaves of a given species are presented. Typical standard deviation is of the order of mean values on E_G and C_Y.

Tree	L (cm)	Λ (cm)	$EI10^{-5}$ (N m^2)	m (g)	Elasto-gravity number E_G	Cauchy number C_y (at 0.1 m/s)	Cauchy number C_y (at 10 m/s)
Apple tree *Malus pumila* 'Jubilé'	2.3	3.6	7.8	0.57	0.060	1.4×10^{-4}	1.4
Apple tree *Malus pumila* 'Arianne'	3.1	5.0	20	1.3	0.10	1.5×10^{-4}	1.5
Apple tree *Malus pumila* 'Golden delicious'	3.2	4.5	13	0.80	0.08	2.2×10^{-4}	2.2
Hazelnut tree *Corylus avellana*	1.9	5.5	4.5	0.75	0.17	7.0×10^{-4}	7.0
Apple tree *Malus pumila* 'Fuji'	3.6	4.4	9.8	0.71	0.11	3.1×10^{-4}	3.1
Plum tree *Prunus salicina*	3.4	5.3	20	1.1	0.10	2.5×10^{-4}	2.5
Cherry tree *Prunus avium* 'Burlat'	5.3	7.1	10	1.3	0.48	1.8×10^{-3}	18
Poplar tree *Populus x. euramericana*	6.0	4.4	7.2	1.6	0.58	7.1×10^{-4}	7.1
Apricot tree *Prunus armeniaca* 'Précoce de Saumur'	3.9	4.3	3.9	1.3	0.55	7.9×10^{-4}	7.9
Apricot tree *Prunus armeniaca* 'Old Variety'	5.8	4.2	1.7	1.1	1.83	2.5×10^{-3}	25

Table 3
Parameters of artificial leaves, Ficus and Apricot leaves, used in the experiment.

Leaf	L (cm)	Λ (cm)	$EI10^{-6}$(SI)	m (g)	β/π –	E_G –
Model 1	1.5	1.7	1.0	0.12	0	0.30
Model 2	2.1	2.4	1.0	0.25	0	1.3
Ficus	2.0	4.3	18	0.4	0.45	0.20
Apricot	4.2	4.5	40	1.3	0.02	0.6

$EI=1.1\times10^{-5}$, and $\beta=0$ or $\beta=0.36\pi$. The inclination of the leaf is measured for several values of the wind velocity. Fig. 6b shows the evolution of the angle ϕ with the flow velocity, represented here in terms of the Cauchy number, Eq. (10).

We may adapt the previous mechanical model to the case of wind loading, Fig. 4b. The force caused by wind is assumed to be normal to the leaf and with a magnitude of $F_n=\rho U^2 C_N S/2$, where ρ is the air density, U is the wind velocity, C_N is the normal drag coefficient (Blevins, 1984), and $S=\Lambda^2\cos\phi$ is the projected area in the wind direction. Hereafter C_N will be taken equal to 1, but may actually depend on ϕ. In a dimensionless form, using $\bar{s}=s/L$, the equation governing the petiole deformation reads

$$\frac{d^2\alpha}{d\bar{s}^2}=\frac{L}{2\Lambda}C_Y C_N\cos\phi\cos(\phi-\alpha). \tag{11}$$

The boundary conditions at the branch side and the lamina side are $\alpha=\theta$ and $d\alpha/d\bar{s}=-C_Y C_N\cos(\phi+\beta)/2$ respectively. The numerical solution to this equation is shown in Fig. 6b, in good agreement with experiments, using $C_N=1$.

A simpler form of the relation between the insertion angle, θ, and the leaf angle, ϕ, may be derived as a function of the Cauchy number. In the limit $\Lambda\gg L$, large leaf or short petiole, and $\phi\approx\pi/2$ the solution reads $\alpha(\bar{s})=\theta-\bar{s}C_Y(\pi/2+\phi)$ so that

$$\phi=\frac{\theta+\beta+\frac{\pi}{2}C_Y}{1+C_Y}. \tag{12}$$

At low C_Y, we have $\phi=\theta$ (unbent petiole) and in the limit of large C_Y, $\phi=\pi/2$ so that the leaf is bent in the wind direction. This approximation is compared with the experimental data in Fig. 6b. This simpler form will be used hereafter.

4. Combined models of leaf inclination angle distribution

4.1. Effects of gravity

We now combine the preceding results on the effect of petiole flexibility, Section 3, with those on the distribution of branch inclinations, Section 2. Considering first gravity, we invert Eq. (9)

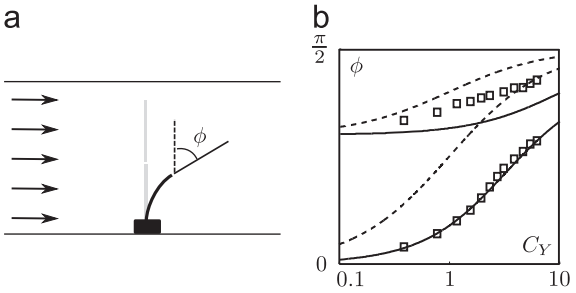

Fig. 6. Schematic view of the experiment in wind tunnel (a). Measured deflection angle, ϕ, as a function of wind speed through the Cauchy number. The solid line corresponds to the elastica model and the dashed line is the analytical approximation.

to express θ as a function of ϕ, and inserting the result in Eq. (4) yields directly the leaf inclination angle distribution as a function of all parameters

$$P(\phi)\propto e^{[-(\phi-\Phi_0)^2/2\Sigma^2]}, \tag{13}$$

where the peak value and the standard deviation are

$$\Phi_0=\frac{\mu+\beta+\pi E_G}{1+E_G},\quad \Sigma=\frac{\sigma}{1+E_G}, \tag{14}$$

where μ and σ are given in Eq. (5). This contains the effect of all parameters on the LIAD, namely the branching angle in the tree, θ_0, the petiole/lamina angle, β, and the combined flexibility/gravity parameter of the leaves, $E_G=mgL\Lambda/EI$. To illustrate this result, several typical LIADs are shown in Fig. 7, resulting from particular choices of the parameters.

We now focus the discussion on the effects of the parameters on the value of the peak of the LIAD, Φ_0, Eq. (14). As noted previously, the effect of the branching angle, θ_0, is rather weak, as shown in Fig. 8a. In particular, the branching angle may not be responsible for a position of the peak of the LIAD larger than $\pi/2$ if $E_G=0$ and $\beta=0$. We shall use hereafter $\theta_0=\pi/3$ unless otherwise noted. The effect of the lamina/petiole angle, β, is simple in the sense that it essentially shifts the peak Φ_0 linearly. The most important parameter in our analysis is the flexibility parameter E_G, which combines the lamina load and the petiole flexibility. This parameter has a strong influence on the LIAD, see Fig. 8b. In the limit of $E_G\ll1$, the LIAD is identical to the BIAD, as the leaves are undeformed by gravity. Conversely when $E_G\gg1$, all the leaves are pointing downward and the LIAD tends to $\Phi_0=\pi$. Typical values of the parameter E_G range from 0.1 to 2, see Table 2. In this range, the LIAD is strongly affected by the flexibility. Note that, for a given tree, changes in flexibility, by growth or dehydration (Faisal et al., 2010; Niklas and Spatz, 2012), may result in a change of LIAD.

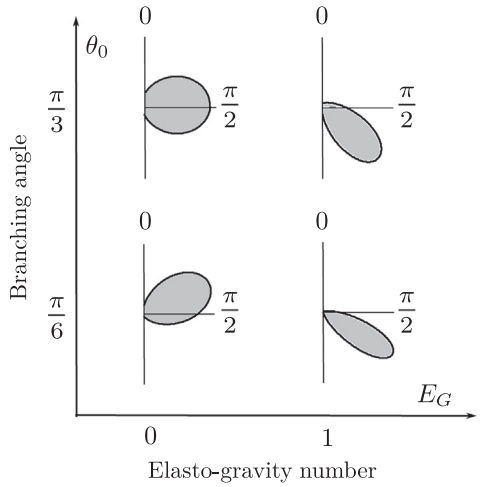

Fig. 7. Computed LIAD showing a strong effect of the elasto-gravity number E_G, for two values of the branching angle, θ_0. Here E_G=0 or 1 and $\theta_0=\pi/6$ or $\pi/3$.

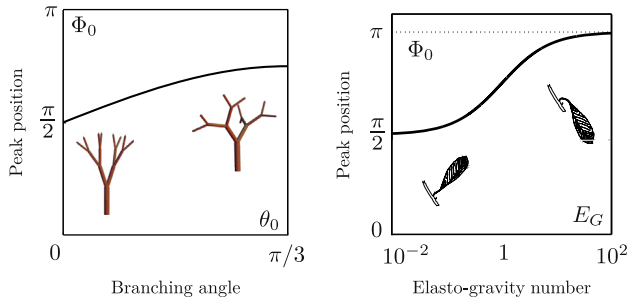

Fig. 8. Dependance of the peak of the LIAD with parameters. (a) Effect of the branching angle of the tree, θ_0, for E_G=1, showing a weak influence. (b) Effect of the elasto-gravity number E_G for $\theta_0=\pi/3$, showing a strong influence.

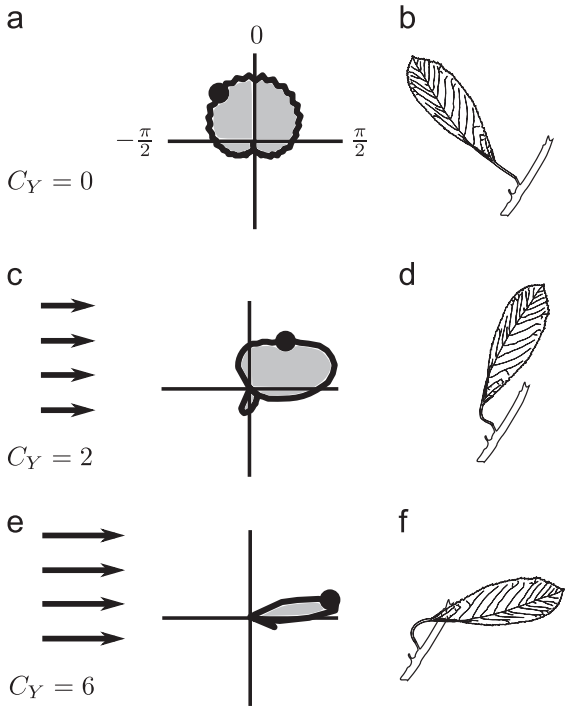

Fig. 9. Evolution of the LIAD with increasing wind velocity. The black dot corresponds to the specific leaf inclination sketched on the right (b, d, f).

4.2. Effects of wind

By combining Eqs. (4) and (12), the LIAD under wind may now be computed. Here, contrary to the case of gravity, the wind loading is sightly more complex as the wind defines a particular direction. Indeed the inclination of leaves are differently affected depending on their orientation with this direction.

A first case may be treated, considering the 2D tree model. It must be kept in mind that the 2D tree model, Section 2.1, bears a caveat as it enforces the peak of the distribution of branch angles to be at θ=0. Yet, it may be readily used to understand qualitatively the effect of wind on a LIAD. Disregarding scaling factors, we use the BIAD given by Eq. (3). Upon inverting the relation between ϕ and θ, Eq. (9), the LIAD may be derived as

$$P(\phi) \propto e^{[-(\phi-\Phi_1)^2/2\Sigma_1^2]}, \tag{15}$$

with $\Phi_1=\pi C_Y/2(1+C_Y)$ and $\Sigma_1=n\theta_0^2/(1+C_Y)^2$. Using the polar representation, Fig. 9 shows that the LIAD, originally symmetric about the vertical angle, becomes skewed in the windward direction, as expected when C_Y is increased. More precisely, all leaves pointing above the axis of wind, that is for θ between $\pi/2$ and $-\pi/2$, Fig. 9, are lifted by wind and ultimately aligned in the direction of wind, $\phi=\pi/2$. Conversely, leaves below the axis of wind are pushed down by wind and finally also aligned downwind, but by going through the down-pointing position. This result shows that, as the Cauchy number is varied, a significant reorganization of the LIAD is expected.

4.3. An application to light interception

As mentioned in the Introduction, the direct light interception by a canopy is linked to the LIAD. More precisely, the simple form of Eq. (1) for a sun at the zenith may be extended to the more general case of a sun time-varying inclination angle $\gamma(t)$ (Pisek et al., 2011; Varlet-Grancher et al., 1993) as

$$\ln\frac{I_0(t)}{I_H(t)} = -A\left[1-\int_0^{\pi/2} P(\varphi)F(\varphi,\gamma)\,\mathrm{d}\varphi\right] \tag{16}$$

where F is given in Pisek et al. (2013). Actually it is more relevant for processes, such as photosynthetic activity, to consider the intercepted light over a full day, as follows: $\int_{Day} I_0(t)\,\mathrm{d}t$. This implies that incoming light dependence on solar inclination is modeled for instance following Campbell and Norman (1998) as

$$I_H(t) \propto 0.7^{1/\sin\,\gamma(t).} \tag{17}$$

In the framework defined above, we may now estimate the effect of the elasto-gravity number, E_G, on the direct light interception as follows: in Eq. (16), the LIAD $P(\varphi)$ now depends on E_G, denoted as $P(\varphi,E_G)$. To quantify this effect, we may define the following light interception correction factor which estimates changes in light interception relatively to the reference case E_G=0:

$$C = \frac{\left[\int_{Day} I_0(t)\,\mathrm{d}t\right]_{E_G}}{\left[\int_{Day} I_0(t)\,\mathrm{d}t\right]_{E_G=0}}, \tag{18}$$

where I_0 is given by Eq. (16), but using $P(\varphi,E_G)$ in place of $P(\varphi)$. This correction factor now only depends on the chosen day, j, the chosen location latitude, λ, which affects $\gamma(t)$, and the elasto-gravity number E_G. To illustrate this effect, we show in Fig. 10 the influence of E_G at the summer solstice and at a latitude of 45°N.

Clearly E_G affects light interception when it comes close to E_G=1 which is a case of practical interest, see Table 2. For large values of E_G, when all leaves hang downwards, a limit value is obtained, C_∞, which only depends on the latitude, for a particular day. As a synthetic result, we show in Fig. 10 this correction factor

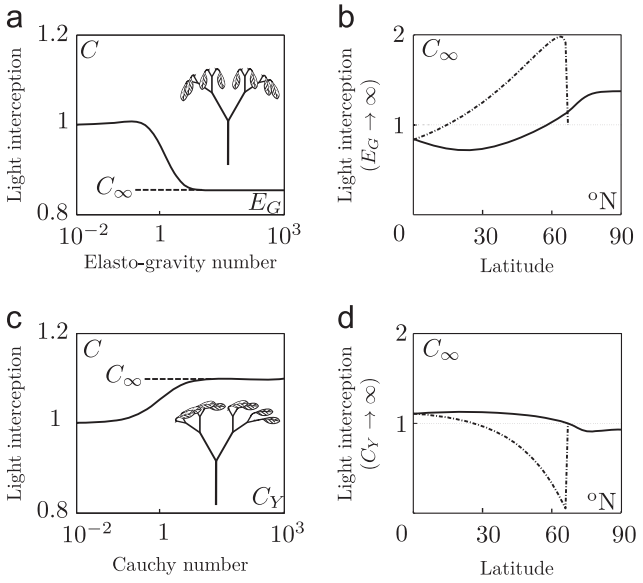

Fig. 10. Effect of the mechanical deformation of the leaves on light interception. (a) Evolution of the correction factor C, Eq. (18), with elasto-gravity number E_G at a latitude 45°N, on summer solstice. (b) Evolution of the limit value C_∞ with the latitude, λ, for summer and winter solstices, continuous line and dashed line respectively. (c) and (d) Same graphs but with wind loading. All calculations are done with $A=3$.

C_∞ as a function of latitude in the Northern Hemisphere at the two solstices. Clearly, the deformation of the petiole affects light interception, but this effect varies significantly with latitude and day in the year. Overall, in the growing season in temperate and equatorial zones, the light interception is reduced by petiole flexibility of 10–20% at most.

Exactly the same procedure may be used to show the effect of wind on light interception through the deformation of the leaves. Yet, wind loading has a preferred direction, which is that of wind. Hence the 2D model given in Section 3 is not sufficient. We improve it as follows: (a) instead of using a simplified Eq. (12), we return to the full equation describing the deformation of the petiole, (b) the loading on a leaf is corrected by a factor $\cos\psi$ where ψ is the azimuth angle of the leaf with respect to wind, and (c) the wind direction is then assumed to be isotropically distributed. By doing so, a correction factor C may be derived, which only depends on day, latitude and Cauchy number. The evolution of C with the Cauchy number is shown in Fig. 10c, for a latitude 45°N at the summer solstice. The light interception is seen to be enhanced by wind. It reaches a plateau, C_∞, for large values of C_Y, when all leaves are horizontal. Fig. 10d shows the evolution of this plateau with the latitude, at summer and winter solstices. At the season of growth, light interception is rather enhanced by wind ($C_\infty > 1$).

5. Discussion and conclusions

We have built up a biomechanical model in order to understand the role of the leaf deformation on the Leaf Inclination Angle Distribution (LIAD). The first issue was to quantify the effect of the tree geometry, characterized essentially by a branching angle and an iterative construction. This allowed to derive the Branch Inclination Angle Distribution (BIAD), which was shown to depend directly on the branching angle. These results were obtained on both 2D and 3D tree geometries, and we have shown that 2D models carry a bias. We have only considered a simplistic tree geometry, in an idealized form of sympodial architectures. We expect that more complex tree architectures, such as a monopodial one (Rodriguez et al., 2008), would lead to different forms of the BIAD, but will have a similar dependence on the branching angle. Similarly, randomness in branching is not expected to change the main conclusion, namely that the peak of the BIAD shifts with the branching angle.

Second, we proposed models for the deformation of a single leaf under gravity or wind loading. These non-linear models are well suited to represent large deflections of the leaf through bending of the petiole. Experiments on real and artificial leaves confirmed their validity. Two dimensionless parameters, the elasto-gravity number E_G and the Cauchy number C_Y, were defined to scale the magnitude of deformations under gravity and wind respectively. Such models may be extended in many directions, at the cost of simplicity by including: (i) other modes of deflection than pure bending, such as torsion (Vogel, 1992), (ii) non-uniform or non-isotropic petiole characteristics (Faisal et al., 2010), (iii) other shapes of leaves (Moulia et al., 1994), (iv) effects of growth on the petiole geometry, and (v) non-linear elastic properties of the petiole. These additional effects will probably change quantitatively the final results of the paper, such as those of Fig. 10, but are not expected to change them qualitatively: the simple models used in this paper showed the direct link between leaf and global parameters. Note that in our approach the elasto-gravity number E_G may change with time for a growing leaf, for instance by change of petiole stiffness due to a change in turgor pressure. Similarly, the Cauchy number may change because of wind velocity but also with petiole stiffness or change of lamina geometry by reconfiguration (Vogel, 1989; Gosselin et al., 2010).

Third, we combined the preceding geometrical and mechanical models to derive the LIAD models. We showed that for small values of E_G and C_Y, the LIAD results directly from the BIAD, and therefore from the branching angle. Conversely, in the limit of large E_G or C_Y, the leaves are fully deformed, and the LIAD is governed by the deformation of the petiole, not the tree geometry.

The main objective of this work was to derive a simple mechanistic model of LIAD changes by gravity and wind loadings. Thus for the sake of simplicity, our elementary biomechanical models do not take into account other factors that are known to affect the LIAD: phototropism, gravitropism or growth history. However all factors affecting LIAD through petiole flexibility such as growth or dehydration (Faisal et al., 2010; Niklas and Spatz, 2012) can be directly handled. The issue of leaf flutter is a bit more complex to take into account for several reasons. First, at the individual leaf level, flutter may correspond to several mechanism of fluid–structure interaction and therefore has a complex dependence on the parameters (Païdoussis et al., 2010). Second, at the tree level, one needs to define a "dynamic" LIAD for the extension of a single leaf flutter amplitude model to the leaf population flutter distribution. Finally, the effect of leaf motion on biological traits such as photosynthesis or water retention is largely unexplored, outside works such as by Roden and Pearcy (1993). Although the effect of wind and flutter on light interception is totally a different issue, our methodology may be of some help to tackle it. Clearly, our approach differs from classical LIAD representations where data are fitted with empirical functions which do not allow predictability. As an application, we have incorporated our LIAD models in the existing computation frameworks of direct light interception, using the approach of Monsi and Saeki (2005) and Pisek et al. (2013). Both gravity and wind were shown to affect light interception, through leaf inclination. The proposed approach seems generic enough to be used in the modeling of many biomechanical effects on statistical populations of leaves in a tree. Results such as those of Niinemets and Fleck (2002) on optimal allocation of biomass in leaves for light interception can probably be extended to more general conditions using the present work.

Acknowledgments

The authors gratefully acknowledge fruitful discussions with Bruno Moulia, Sarah Puijalon and Christophe Eloy and thank Daniel Falster for communicating detailed experimental data and Pascal Hémon for help on the design of experiments.

References

Blevins, R., 1984. Applied Fluid Dynamics Handbook, vol. 1.
Campbell, G., 1986. Extinction coefficients for radiation in plant canopies calculated using an ellipsoidal inclination angle distribution. Agricultural and Forest Meteorology 36, 317–321.
Campbell, G., Norman, J., 1998. Introduction to Environmental Biophysics. Springer Verlag.
Eloy, C., 2011. Leonardo's rule, self-similarity, and wind-induced stresses in trees. Physical Review Letters 107, 258101.
Faisal, T.R., Khalil Abad, E., Hristozov, N., Pasini, D., 2010. The impact of tissue morphology, cross-section and turgor pressure on the mechanical properties of the leaf petiole in plants. Journal of Bionic Engineering 7, S11–S23.
Falster, D., 2012. Private Communication.
Falster, D.S., Westoby, M., 2003. Leaf size and angle vary widely across species: what consequences for light interception? New Phytologist 158, 509–525.
Gosselin, F., de Langre, E., Machado-Almeida, B., 2010. Drag reduction of flexible plates by reconfiguration. Journal of Fluid Mechanics 650, 319–341.
Kittel, C., 2004. Elementary Statistical Physics. Courier Dover Publications.
de Langre, E., 2008. Effects of wind on plants. Annual Review of Fluid Mechanics 40, 141–168.
Lemaitre, C., Hémon, P., de Langre, E., 2005. Instability of a long ribbon hanging in axial air flow. Journal of Fluids and Structures 20, 913–925.
Lopez, D., 2011. Flow-induced pruning of branched systems and brittle reconfiguration. Journal of Theoretical Biology 284, 117–124.
Monsi, M., Saeki, T., 2005. On the factor light in plant communities and its importance for matter production. Annals of Botany 95, 549–567.
Moulia, B., Fournier, M., Guitard, D., 1994. Mechanics and form of the maize leaf: in vivo qualification of flexural behaviour. Journal of Materials Science 29, 2359–2366.
Niinemets, Ü., Fleck, S., 2002. Petiole mechanics, leaf inclination, morphology, and investment in support in relation to light availability in the canopy of *Liriodendron tulipifera*. Oecologia 132, 21–33.
Niklas, K., 1992. Plant Biomechanics: An Engineering Approach to Plant Form and Function. University of Chicago Press.
Niklas, K., 1999. A mechanical perspective on foliage leaf form and function. New Phytologist 143, 19–31.
Niklas, K., Spatz, H.C., 2012. Plant Physics. University of Chicago Press.
Païdoussis, M., Price, S., De Langre, E., 2010. Fluid–Structure Interactions: Cross-Flow-Induced Instabilities. Cambridge University Press.
Pisek, J., Ryu, Y., Alikas, K., 2011. Estimating leaf inclination and *g*-function from leveled digital camera photography in broadleaf canopies. Trees 25, 919–924.
Pisek, J., Sonnentag, O., Richardson, A., Mõttus, M., 2013. Is the spherical leaf inclination angle distribution a valid assumption for temperate and boreal broadleaf tree species? Agricultural and Forest Meteorology 169, 186–194.
Roden, J., Pearcy, R., 1993. Effect of leaf flutter on the light environment of poplars. Oecologia 93, 201–207.
Rodriguez, M., de Langre, E., Moulia, B., 2008. A scaling law for the effects of architecture and allometry on tree vibration modes suggests a biological tuning to modal compartmentalization. American Journal of Botany 95, 1523–1537.
Rodriguez, M., Ploquin, S., Moulia, B., de Langre, E., 2012. The multimodal dynamics of a walnut tree: experiments and models. Journal of Applied Mechanics 79, 4505.
Salençon, J., 2001. Handbook of Continuum Mechanics. General Concepts. Thermoelasticity. Springer, Berlin.
Varlet-Grancher, C., Bonhomme, R., Sinoquet, H., et al., 1993. Crop Structure and Light Microclimate: Characterization and Applications. INRA Editions.
Vogel, S., 1989. Drag and reconfiguration of broad leaves in high winds. Journal of Experimental Botany 40, 941–948.
Vogel, S., 1992. Twist-to-bend ratios and cross-sectional shapes of petioles and stems. Journal of Experimental Botany 43, 1527–1532.
Wang, W.M., Li, Z.L., Su, H.B., 2007. Comparison of leaf angle distribution functions: effects on extinction coefficient and fraction of sunlit foliage. Agricultural and Forest Meteorology 143, 106–122.